Imaging the quark and gluon substructure of the pion

Minghui Ding

Helmholtz-Zentrum Dresden-Rossendorf, Institute of Theoretical Physics, Dresden, Germany

December 6th, 2023

Polish-German WE-Heraeus Seminar & Max Born Symposium
Many-Particle Systems under Extreme Condition, Synagoge Görlitz, December 3-6, 2023

The pion

Naive picture: π^+
up quark + down antiquark:

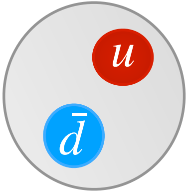

Realistic picture: π^+
up quark + down antiquark + sea quarks + gluons

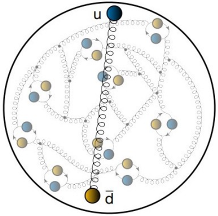

Nambu-Goldstone bosons of spontaneously broken chiral symmetry.

Mass: ~ 140 MeV; the lightest hadron; spin 0; P parity $-$; pseudoscalar meson.

Nambu-Goldstone boson

Pion does not fit naturally into the mass pattern of constituent quark model:

Maris, Roberts, Tandy, Phys. Lett. B 420 (1998) 267-273.

$$f_\pi m_\pi^2 = 2 m_u \rho_\pi \tag{1}$$

f_π, leptonic decay constant; m_π, pion mass; m_u, current quark mass; ρ_π, pseudoscalar projection of the pion wave function onto the origin in configuration space.

- Gell-Mann-Oakes-Renner (GMOR) relation.
- Pion mass m_π vanishes in the absence of current quark mass m_u - Nambu-Goldstone boson of chiral symmetry breaking (when current quark mass is zero, QCD Lagrangian possesses a chiral symmetry).
- Mass square of pion rises linearly with the current quark mass, $m_\pi^2 \propto m_u$, whereas in constituent quark model $m_{\text{meson}} \propto m_{\text{quark}}$.

Nambu-Goldstone boson

Axial-vector Ward-Takahashi identity in chiral limit: $\mathcal{M}^{ab} = 0$; anomaly: $\mathcal{A}^a(k;P) = 0$.

$$P_\mu \Gamma^a_{5\mu}(k;P) = \mathcal{S}^{-1}(k_+) i\gamma_5 \mathcal{F}^a + i\gamma_5 \mathcal{F}^a \mathcal{S}^{-1}(k_-) \tag{2}$$

Quark propagator: $S^{-1}(k) = i\gamma\cdot k A(k^2) + B(k^2)$, right hand side:

$$\lim_{P^2\to 0} R = i\gamma_5 B(k^2)\,, \tag{3}$$

Massless pion pole in axial vector vertex: $\Gamma_{5\mu}(k,P) \xrightarrow{P^2=-m_\pi^2} \frac{f_\pi P_\mu}{P^2+m_\pi^2}\Gamma_\pi(k;P)$, left hand side:

$$\lim_{P^2\to 0} L = i\gamma_5 f_\pi E_\pi(k;P=0)\,, \tag{4}$$

Compare Eq.(3) and Eq.(4)

$$f_\pi E_\pi(k;P=0) = B(k^2)\,. \tag{5}$$

Nambu-Goldstone boson

Pion's Goldberger-Treiman relation: Maris, Roberts, Tandy, Phys. Lett. B 420 (1998) 267-273.

$$f_\pi E_\pi(k; P=0) = B(k^2) \tag{6}$$

Pion's Bethe-Salpeter amplitude, solution of the Bethe-Salpeter equation

$$\Gamma_\pi(k;P) = \gamma_5[iE_\pi(k;P) + \gamma\cdot P F(k;P) + \gamma\cdot k k\cdot P G(k;P) + \sigma_{\mu\nu}k_\mu P_\nu H(k;P)] \tag{7}$$

Dressed-quark propagator

$$S^{-1}(k) = i\gamma\cdot k A(k^2) + B(k^2) \tag{8}$$

Dynamical chiral symmetry breaking (DCSB) $\Leftrightarrow$ Goldstone theorem

- Pion exists if, and only if, mass is dynamically generated
- Algebraically explain why pion is massless in the chiral limit
- Two body problem is solved, almost completely, once solution of one body problem is known

One-Body Matter Sector

Two body problem is solved, almost completely, once solution of one body problem is known. Quark propagator:

$$S(k;\zeta) = \frac{1}{i\gamma\cdot k A(k^2;\zeta) + B(k^2;\zeta)} = \frac{Z(k^2;\zeta)}{i\gamma\cdot k + M(k^2)} \tag{9}$$

- Massless partonic quarks acquire a momentum dependent mass function which is large at infrared momenta.
- This mass scale is responsible for all hadron masses.
- Properties of the nearly massless pion are the clearest window onto emergence of hadron mass (EHM) in the Standard Model.

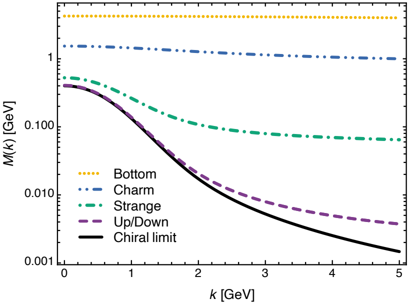

Roberts, Richards, Horn, Chang, Prog. Part. Nucl. Phys. 120 (2021) 103883.

The structure of pion

Form factor: the closest thing we have to a snapshot, the size, shape and makeup of pion

- Electromagnetic form factor
- Two-photon transition form factor
- Gravitational form factor

1D picture of how quarks move within pion

- Parton distribution amplitude
- Parton distribution function (PDF)

A multidimensional view of pion structure

- Transverse momentum dependent distribution function (TMD)
- Generalized parton distribution (GPD)

HELMHOLTZ ZENTRUM DRESDEN ROSSENDORF

Part I

Form factor: the closest thing we have to a snapshot, the size, shape and makeup of pion.

Form factors

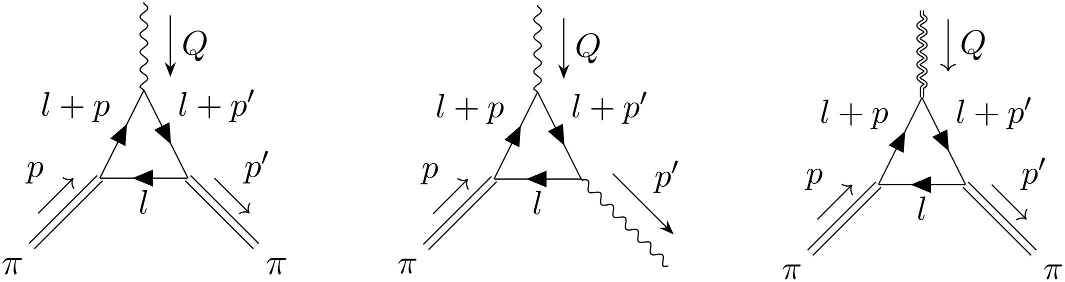

(1) electromagnetic form factor; (2) two-photon transition form factor; (3) gravitational form factor.

Electromagnetic form factor

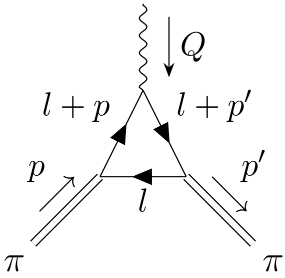

Figure: Feynman diagram for $\pi^+(p) \to \pi^+(p')$ elastic electromagnetic form factor $F_\pi(Q^2)$.

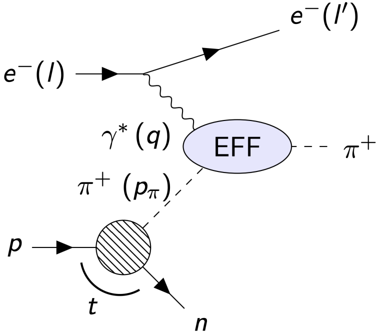

Figure: No free pion target - use "virtual pion cloud" of the proton.

Electromagnetic form factor: small Q^2

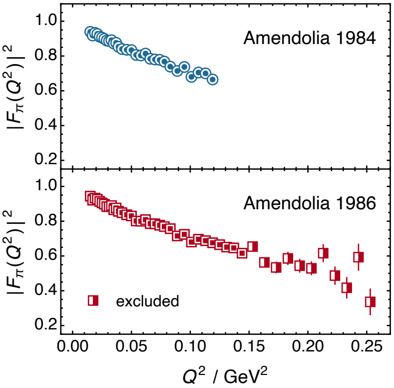

Figure: Data collected at CERN by the NA7 Collaboration.

Cui, Binosi, Roberts, Schmidt, Phys. Lett. B 822 (2021) 136631.

Electric radius-squared is obtained from the slope of the form factor at $Q^2 = 0$,

$$r_\pi^2 = -\frac{6}{F_\pi(0)} \frac{d}{dQ^2} F_\pi(Q^2)\Big|_{Q^2=0}, \tag{10}$$

and $r_\pi \approx 0.640(7)$ fm.

Electromagnetic form factor: large Q^2

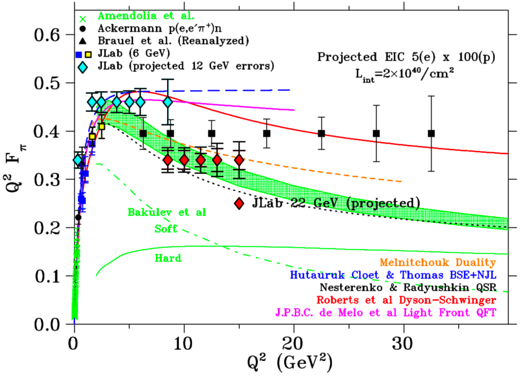

- $Q^2F_\pi(Q^2)$, figure is taken from JLab 22 GeV white paper (arXiv:2306.09360 [nucl-ex]).
- Existing data (blue, black, yellow, green) and projected uncertainties for future data on the pion form factor from JLab (12 GeV: cyan; 22 GeV: red) and EIC (black), in comparison to a variety of hadronic structure models. Dyson-Schwinger Equation:

Chang, Cloët, Roberts, Schmidt, Tandy, Phys. Rev. Lett. 111 (2013) 14, 141802. Chen, Ding, Chang, Roberts, Phys. Rev. D 98 (2018) 9, 091505.

Two-photon transition form factor

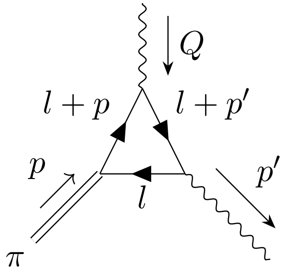

Figure: Feynman diagram for $\gamma\gamma^* \to \pi^0$, neutral pion electromagnetic transition form factor $G_\pi(Q^2)$.

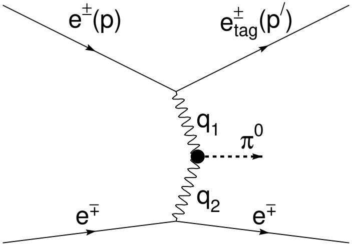

Figure: Single-tagged mode: $q_1^2 \neq 0, q_2^2 \approx 0$.

Two-photon transition form factor

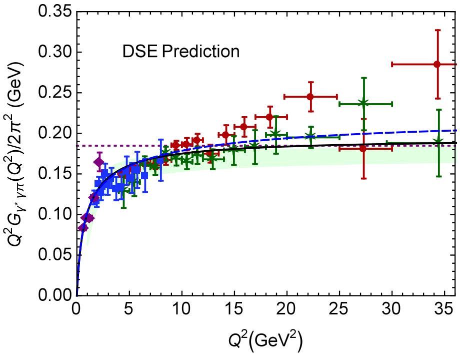

Figure: Data: CELLO - diamonds (purple); CLEO -squares (blue); BaBar - circles (red); Belle - stars (green). Our results favor the Belle data, The situation may be clarified by upcoming data from BelleII.

Raya, Chang, Bashir, Cobos-Martinez, Gutiérrez-Guerrero, Roberts, Tandy, Phys. Rev. D 93 (2016) 7, 074017. Eichmann, Fischer, Weil, Williams, Phys. Lett. B 774 (2017) 425-429.

Gravitational form factor

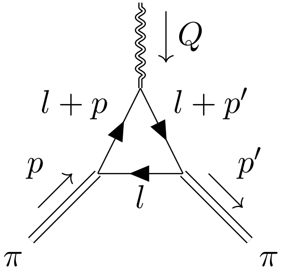

Figure: Feynman diagram for pion gravitational form factors.

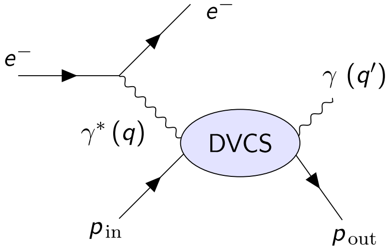

Figure: Deep Virtual Compton Scattering (DVCS).

No direct way to measure the hadron gravitational form factor, but it may be probed indirectly in DVCS, through its connection with generalized parton distributions (GPDs):
$\int_{-1}^{1} dx\, x\, H^q(x,\xi,Q^2) = A^q(Q^2) + \xi^2 D^q(Q^2)$.

Gravitational form factor

The gravitational form factors of pion can be extracted from its matrix elements of the energy-momentum tensor (EMT)

$$\langle p'|T^{\mu\nu}|p\rangle = M^{\pi}_{\mu\nu}(Q^2) = 2P_\mu P_\nu A(Q^2) + \frac{1}{2}\left(Q_\mu Q_\nu - Q^2\delta_{\mu\nu}\right) D(Q^2) + 2m_\pi^2\delta_{\mu\nu}\bar{c}(Q^2)\,, \tag{11}$$

D-term: form factor at $Q^2 = 0$, i.e., $D \equiv D(0)$.

- Global property, just like electric charge, magnetic moment, mass, spin etc.
- Always negative, Goldstone boson in the soft-pion limit: $D = -1$.

Gravitational form factor $A(Q^2)$ and $D(Q^2)$: define the mass radius and pressure distribution radius

$$r_A^2 = -\frac{6}{A_\pi(0)}\,\frac{d}{dQ^2}A_\pi(Q^2)\Big|_{Q^2=0}\,, \qquad r_D^2 = -\frac{6}{D_\pi(0)}\,\frac{d}{dQ^2}D_\pi(Q^2)\Big|_{Q^2=0}\,. \tag{12}$$

Recent analysis yields $r_A = 0.51(2)$ fm, and $r_D = 0.80(4)$ fm, recall charge radius $r_F \approx 0.640(7)$ fm. The mass radius is predicted to be somewhat smaller than its charge radius. Xu et al, Chin. Phys. Lett. 40 (2023) 4, 041201.

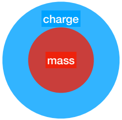

HZDR
HELMHOLTZ ZENTRUM DRESDEN ROSSENDORF

Part II

1D picture of how quarks move within pion

Parton distribution amplitude

Large-Q^2 behaviour of pion electromagnetic form factor is predicted by perturbative QCD (pQCD) analyses as:

$$\exists Q_0 > \Lambda_{\rm QCD} \mid Q^2 F_\pi(Q^2) \stackrel{Q^2 > Q_0^2}{\approx} 16\pi\alpha_s(Q^2) f_\pi^2 w_\varphi^2(Q^2), \tag{13}$$

where: f_π is the pion's leptonic decay constant; $\alpha_s(Q^2)$ is the strong running-coupling, and

$$w_\varphi(Q^2) = \frac{1}{3}\int_0^1 dx\, \frac{1}{x}\varphi_\pi(x;Q^2)\,, \tag{14}$$

where $\varphi_\pi(x;Q^2)$ is the pion's valence-quark leading-twist parton distribution amplitude (PDA). On the domain $\Lambda_{\rm QCD}^2/Q^2 \simeq 0$,

$$\varphi_\pi(x;Q^2) \stackrel{\Lambda_{\rm QCD}^2/Q^2 \simeq 0}{\approx} \varphi_\pi^{\rm cl}(x) = 6x(1-x)\,; \tag{15}$$

and hence

$$Q^2 F_\pi(Q^2) \stackrel{\Lambda_{\rm QCD}^2/Q^2 \simeq 0}{\approx} 16\pi\alpha_s(Q^2) f_\pi^2\,. \tag{16}$$

Parton distribution amplitude

Dyson-Schwinger Equation: Chang, Cloet, Cobos-Martinez, Roberts, Schmidt, Tandy, Phys. Rev. Lett. 110 (2013) 13, 132001.

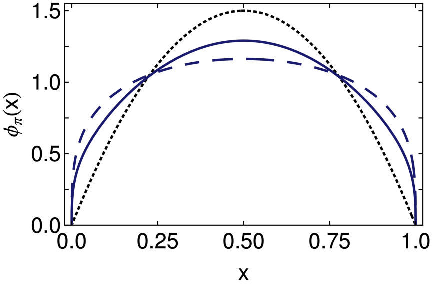

Figure: Curves: solid, DCSB-improved kernel (DB); dashed, rainbow ladder (RL); and dotted, asymptotic distribution.

Lattice QCD with Large Momentum Effective Theory (LaMET) approach:

Zhang, Honkala, Lin, Chen, Phys. Rev. D 102, 094519 (2020).

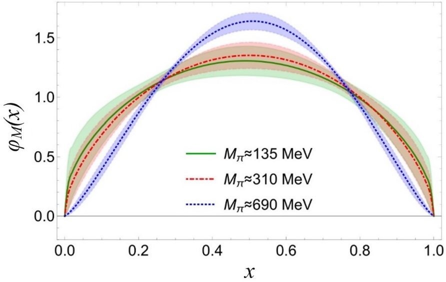

Parton distribution amplitude

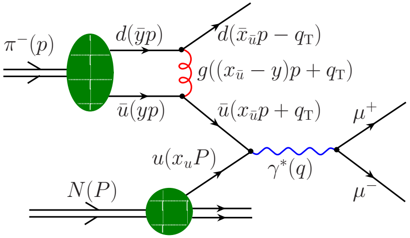

Figure: Graphical representation of the Drell-Yan process $\pi^- N \to \mu^+\mu^- X$.

Xing, Ding, Cui, Pimikov, Roberts, Schmidt, arXiv:2308.13695 [hep-ph].

- Using a reaction model, the differential cross-section takes the form

$$\frac{d^5\sigma(\pi^- N \to \mu^+\mu^- X)}{dQ^2 dQ_T^2 dx_L d\cos\theta d\phi} \propto N(\tilde{x}, \rho)$$
$$\times \Big[1 + \lambda \cos^2\theta + \mu \sin 2\theta \cos\phi + \tfrac{1}{2}\nu \sin^2\theta \cos 2\phi$$
$$+ \bar{\mu} \sin 2\theta \sin\phi + \tfrac{1}{2}\bar{\nu} \sin^2\theta \sin 2\phi\Big] \,,$$

  the last line contributes when the nucleon target is longitudinally polarized and is otherwise absent.

- Angular distribution parameters λ, μ, ν (unpolarized target) and $\bar{\mu}, \bar{\nu}$ (longitudinally polarized proton) depend on pion parton distribution amplitude.

Parton distribution function

Synergy

- Experiments:
  - In the past: awarded a high priority – Led to
    (i) the discovery of quarks;
    (ii) Nobel prizes for the experiment leaders;
    (iii) the development of quantum chromodynamics (QCD)
  - Ongoing and in plan:
    Proposals at Jefferson Lab 22 GeV; CERN: COMPASS++/AMBER; Electron Ion Collider (EIC) in USA; Electron-ion collider in China (EicC).
- Global fits:
  Inferred from data, results viewed as benchmarks
- Continuum methods and Lattice QCD:
  Historically, yielded only low-order Mellin moments. Pointwise behavior was not accessible.

Parton distribution function

Theoretical framework in continuum Schwinger function methods

- Concept (I): at a hadron scale ζ_H, dressed valence-quarks carry all the pion's light-front momentum and the glue and sea distributions vanish.

Ding, Raya, Binosi, Chang, Roberts, Schmidt, Phys. Rev. D 101 (2020) 5, 054014

$$\mathfrak{u}^{\pi}(1-x,\zeta_H) = \mathfrak{u}^{\pi}(x,\zeta_H) \tag{17}$$

- Numerically solve the bound-state equations to calculate valence distribution at hadron scale.
- Concept (II): a proposition, there exists an effective charge, $\alpha_{1l}(k^2)$, that, when used to integrate the one-loop pQCD Dokshitzer-Gribov-Lipatov-Altarelli-Parisi (DGLAP) equations, defines an evolution scheme for parton PDFs that is all-orders exact.

Raya, Cui, Chang, Morgado, Roberts, Rodríguez-Quintero, Chin. Phys. C 46 (2022) 1, 013105.

$$\frac{\langle x^n q^M \rangle_\zeta}{\langle x^n q^M \rangle_{\zeta_H}} = \exp\left[\frac{\gamma_0^n}{4\pi}\int_{\ln\zeta^2}^{\ln\zeta_H^2} d(\ln k^2)\,\hat{\alpha}(\ln k^2)\right] \tag{18}$$

- Evolve parton distribution function from hadron scale ζ_H to any other scale ζ.

PDF at hadron scale

Leading-twist valence quark PDF in the operator representation:

$$q(x) = \frac{1}{4\pi}\int dz^- e^{-ixP^+z^-}\langle P|\bar{\psi}(z^-)U^{-\dagger}_{(+\infty;z)}\gamma^+U^-_{(+\infty;0)}\psi(0)|P\rangle\,, \tag{19}$$

Light-cone gauge: $n\cdot A = 0$, Wilson line $U^{-\dagger}_{(+\infty;z)} = U^-_{(+\infty;0)} = 1$. In the parton model,

$$q(x) = \int\frac{d^4k}{(2\pi)^4}\delta\left(n\cdot k - xn\cdot P\right)\,\mathrm{Tr}\left[i\gamma\cdot n\,G(k,P)\right]\,. \tag{20}$$

Pion PDF at hadron scale:

$$q^\pi(x;\zeta_H) = N_c\mathrm{tr}\int_{dk}\delta^x_n(k_\eta)\;n\cdot\partial_{k_\eta}\left[\Gamma_\pi(k_\eta,-P;\zeta_H)S(k_\eta)\right]\Gamma_\pi(k_{\bar{\eta}},P)\,S(k_{\bar{\eta}})\,, \tag{21}$$

$S(k)$, quark propagator; $\Gamma_\pi(k,P;\zeta_H)$, pion Bethe-Salpeter amplitude.

Continuum Schwinger function Methods

One-particle Schwinger function

- Green function of different order couples to each other - truncation
- Some equations are extremely complicated - modeling
- Non-perturbative approach

Eichmann, arXiv:0909.0703.

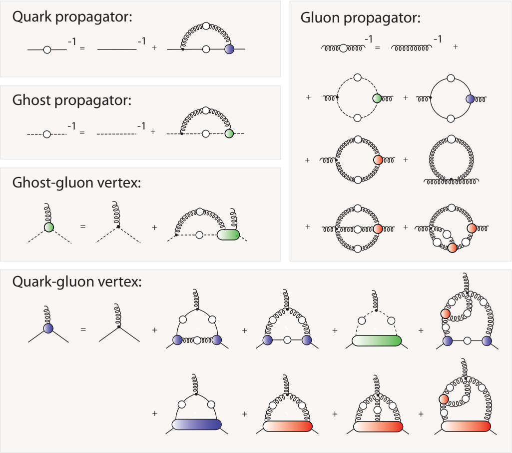

Continuum Schwinger function Methods

Two-particle Schwinger function

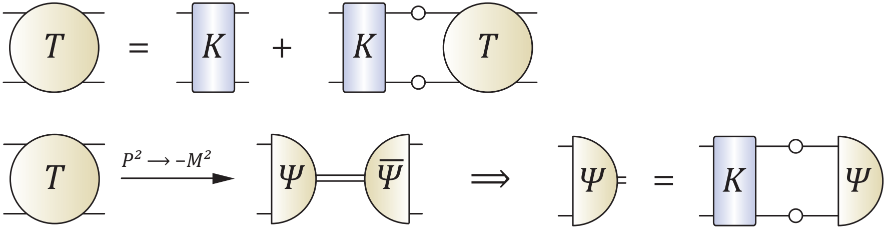

- The two-particle propagator can be expressed in terms of pole contributions, and the residue is the Bethe-Salpeter wave function.
- Bethe-Salpeter Equation.

PDF at hadron scale

- Solid navy curve:
  $q^\pi(x;\zeta_H) = 213.32\,x^2(1-x)^2[1 - 2.9342\sqrt{x(1-x)} + 2.2911\,x(1-x)]\,,$
- long-dashed green curve:
  $q^\pi_{\tilde{\varphi}^2}(x;\zeta_H) = 301.66x^2(1-x)^2[1 - 2.3273\sqrt{x(1-x)} + 1.7889\,x(1-x)]^2\,.$
- Dotted black curve: scale free result
  $q_{\rm sf}(x) = 30x^2(1-x)^2$.
- A broad function, induced by dynamical chiral symmetry breaking.
- Large x behaviour: $q^\pi(x;\zeta_H) \sim (1-x)^2$.

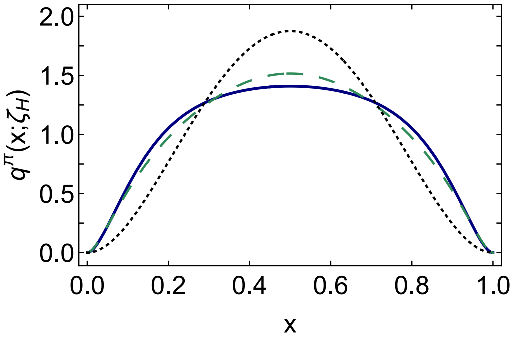

PDF evolution

- Existing Lattice QCD calculations of low-order moments and phenomenological fits to pion parton distributions are typically quoted at $\zeta_2 = 2$ GeV, evolving $q^\pi(x;\zeta_H) \to q^\pi(x;\zeta_2)$.
- Experiment takes the average scale $\zeta_5 = 5.2$ GeV, evolving $q^\pi(x;\zeta_H) \to q^\pi(x;\zeta_5)$.
- Proposition: There exists an effective charge, $\alpha_{1l}(k^2)$, that, when used to integrate the one-loop pQCD DGLAP equations, defines an evolution scheme for parton PDFs that is all-orders exact. $\alpha_{1l}(k^2)$ need not be unique (We use process-independent charge here).

Valence quark distribution PDF Mellin moments: Raya, Cui, Chang, Morgado, Roberts, Rodríguez-Quintero, Chin. Phys. C 46 (2022) 1, 013105.

$$\frac{\langle x^n q^M\rangle_\zeta}{\langle x^n q^M\rangle_{\zeta_H}} = \exp\left[\frac{\gamma_0^n}{4\pi}\int_{\ln\zeta^2}^{\ln\zeta_H^2} d(\ln k^2)\,\hat{\alpha}(\ln k^2)\right], \tag{22}$$

Sea quark and gluon PDF Mellin moments: (generated by valence PDF at hadron scale)

$$\begin{pmatrix}\langle x^n\rangle_\Sigma^\zeta \\ \langle x^n\rangle_g^\zeta\end{pmatrix} = \begin{pmatrix}\alpha_+^n S_-^n + \alpha_-^n S_+^n \\ \beta_{g\Sigma}^n\left(S_-^n - S_+^n\right)\end{pmatrix}\begin{pmatrix}\langle x^n\rangle_\Sigma^{\zeta_H} \\ 0\end{pmatrix}. \tag{23}$$

PDF at $\zeta_5 = 5.2$ GeV

Continumm, Lattice and Experiment

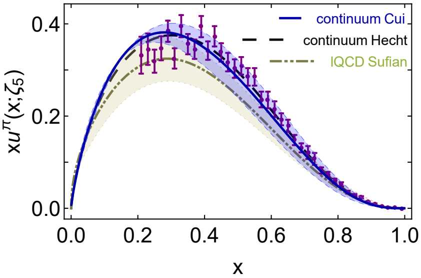

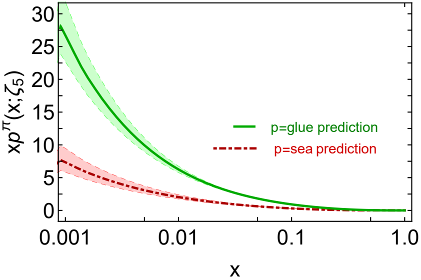

- Within uncertainties, recent continuum valence distribution (Cui) agrees with continuum in 2001 (Hecht), lattice (Sufian), and rescaled E615 experiment data. Conway et al.. Phys. Rev. D 39 (1989) 92-122. Hecht et al.. Phys. Rev. C 63, 025213 (2001). Aicher et al.. PRL 105, 252003 (2010). Sufian et al.. Phys. Rev. D 99, 074507 (2019). Cui et al., Eur. Phys. J. C 80, 1064 (2020).
- Mellin moments: $\langle 2xu^\pi(x;\zeta_5)\rangle = 0.40(2)\,,\ \langle x\rangle_g^\pi = 0.45(2)\,, \langle x\rangle_{\rm sea}^\pi = 0.14(2)\,.$

PDF at $\zeta_5 = 5.2$ GeV

Phenomenological fits

Phenomenological fits update PDFs by including next-to-leading-logarithm (NLL) re-summation effect.

- Double Mellin - does not yield appropriate PDFs at hadron scale.
- Mellin-Fourier - yield PDFs in agreement with $(1-x)^{\beta=2+\gamma}$ behavior at large x .

  Barry, Ji, Sato, Melnitchouk, Phys. Rev. Lett. 127 (23) (2021) 232001. Cui et al. Eur. Phys. J. A 58 (2022) 1, 10.

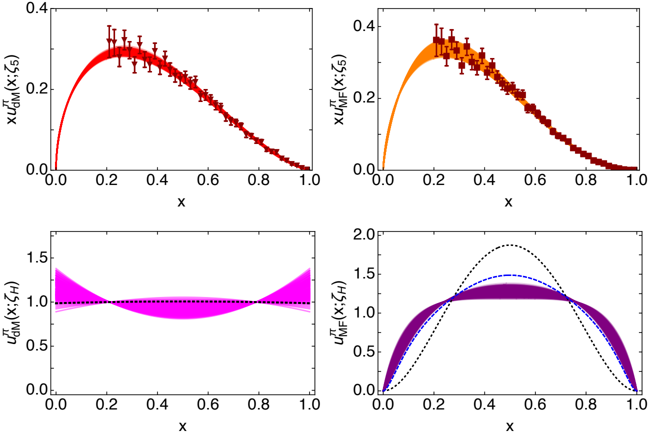

PDF at $\zeta_5 = 5.2$ GeV

Continumm and Lattice

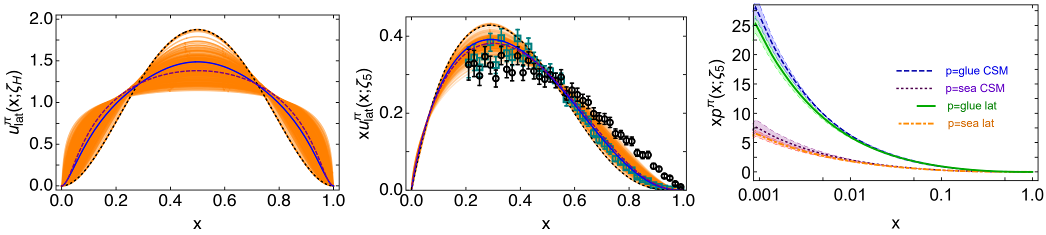

- Exploiting contemporary results from numerical simulations of lattice-regularised QCD, parameter-free predictions for pion valence, glue, and sea PDFs are obtained.

Cui et al. Phys. Rev. D 105 (2022) 9, L091502.

PDF moments

Continuum and Lattice

- Supposing only that there is an effective charge which defines an evolution scheme for PDFs that is all-orders exact, strict lower and upper bounds on all Mellin moments of the valence-quark PDFs of pion-like systems are derived.
- Lattice moments fall within the open band. Joó, Karpie, Orginos, Radyushkin, Richards, Sufian, Zafeiropoulos, Phys. Rev. D 100 (2019) 114512. Sufian, Karpie, Egerer, Orginos, Qiu, Richards, Phys. Rev. D 99 (2019) 074507. Alexandrou, Bacchio, Cloet, Constantinou, Hadjiyiannakou, Koutsou, Lauer, Phys. Rev. D 104 (5) (2021) 054504. Cui et al. Phys. Rev. D 105 (2022) 9, L091502.

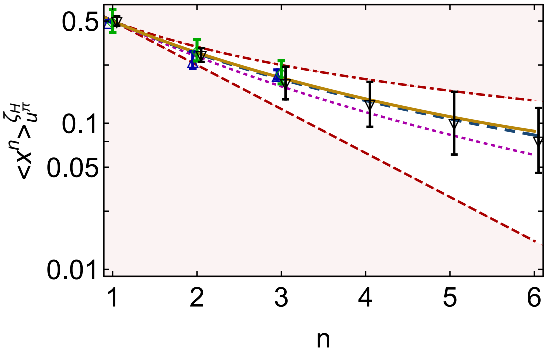

PDF moments

Mathematics and Lattice

- Truncated Hausdorff moment problem
  $s_k = \int_0^1 x^k f(x)\,dx$.
- Necessary and sufficient conditions for the existence of a positive $f(x)$:

$$(s_{i+j})_{i,j=0}^{n} \succeq 0\,,$$
$$(s_{i+j+1} - s_{i+j+2})_{i,j=0}^{n-1} \succeq 0\,; \qquad (24)$$

for the odd case $m = 2n+1$,

$$(s_{i+j+1})_{i,j=0}^{n} \succeq 0\,,$$
$$(s_{i+j} - s_{i+j+1})_{i,j=0}^{n} \succeq 0\,. \qquad (25)$$

$(s_{i+j})_{i,j=0}^{n}$ represents the Hankel matrix.

- Continuity, unimodality, symmetry of $f(x)$ strengthen the sieve.

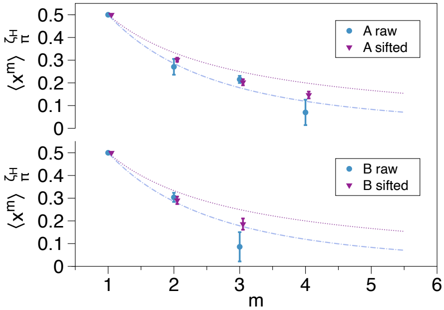

Figure: Through an error-inclusive sifting process, we refine three sets of PDF moments from Lattice QCD. This refinement significantly reduces the errors, particularly for high order moments. Wang, Ding, Chang, arXiv:2308.14871

Part III

A multidimensional view of pion structure

Transverse momentum dependent distribution function

Transverse momentum dependent (TMD) distribution function

- Longitudinal momentum x, transverse momentum k_T.

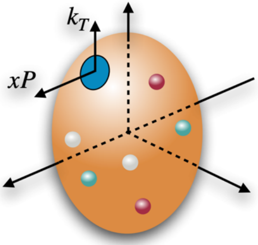

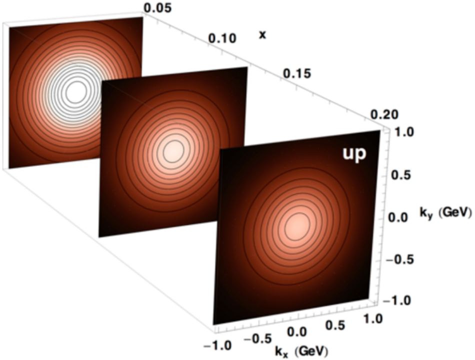

Transverse momentum dependent distribution function

Transverse momentum dependent (TMD) distribution function

- Semi-inclusive deep inelastic scattering (SIDIS)
- Hadron tensor and correlation function
- Transverse momentum dependent
- Wilson line, process-dependent, not universal

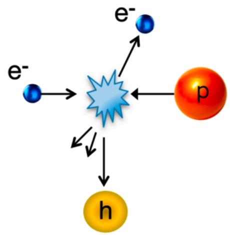

Gauge-invariant TMD correlation function

Bacchetta, Trento lectures, 2012; Mulders, lectures at the Galileo Galilei Institute (2015).

$$\Phi(x, k_\perp) = \int \frac{d^3 r}{8\pi^3} e^{-ixP^+ r^- + ik_\perp \cdot r_\perp} \langle P|\bar{\psi}(0^+, r^- r_\perp) \widetilde{U^\dagger_{(+\infty;r)}} \widetilde{U_{(+\infty;0)}} \psi(0)|P\rangle \,,$$

$$\begin{aligned} \widetilde{U^\dagger_{(+\infty;r)}} &= U^\perp_{(+\infty^-, +\infty_\perp; +\infty^-, 0_\perp)} U^-_{(+\infty^-, 0_\perp; 0^-, 0_\perp)} \,, \\ \widetilde{U_{(+\infty;0)}} &= U^{-\dagger}_{(+\infty^-, r_\perp; r^-, r_\perp)} U^{\perp\dagger}_{(+\infty^-, +\infty_\perp; +\infty^-, r_\perp)} \,. \end{aligned} \tag{26}$$

Transverse momentum dependent distribution function

A valid representation of the Wilson line

- Its contribution is essential to any nonzero result for many interesting (T-odd) TMDs
- A non-perturbative approximation to the Wilson line is obtained via a planar sum of all single gluon interactions between the target remnant and the struck quark.

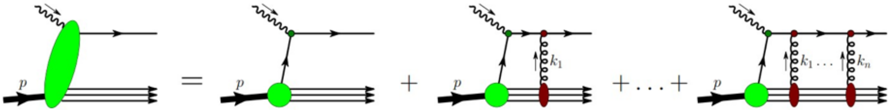

- Boer-Mulders function:
  - Transversely polarized quark in an unpolarized hadron
  - SIDIS experiments such as ZEUS and H1 at DESY, e^+e^- annihilation experiments etc.
- Work in progress ...

Generalized parton distribution

Connection with electromagnetic form factor (0-th Mellin moment of GPD)

Mezrag, Few Body Syst. 63 (2022) 3, 62.

$$\int_{-1}^{1} dx\, H^q(x,\xi,Q^2) = F_{\mathrm{em}}(Q^2)\,, \tag{27}$$

Connection with gravitational form factor (1st Mellin moment of GPD)

$$\int_{-1}^{1} dx\, x\, H^q(x,\xi,Q^2) = A^q(Q^2) + \xi^2 D^q(Q^2)\,, \tag{28}$$

Connection with parton distribution amplitude (in the limit $(\xi,Q^2) \to (1,0)$)

$$H^q(x,1,0) + H^q(-x,1,0) = \varphi\left[(1+x)/2\right]\,, \tag{29}$$

Connection with parton distribution function (forward limit $(\xi,Q^2) \to (0,0)$)

$$H^q(x,0,0) = q(x)\Theta(x) - \bar{q}(-x)\Theta(-x)\,. \tag{30}$$

Generalized parton distribution

GPD measurements: (DVCS, TCS, DVMP)

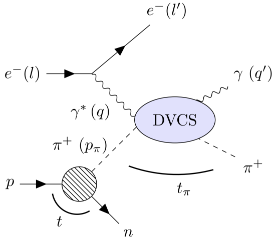

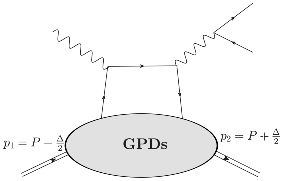

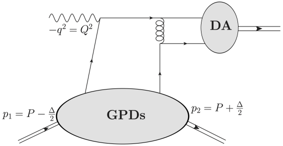

GPD modelling:

- Overlap representation of the light front wave function

  Diehl, Feldmann, Jakob, Kroll, Nucl. Phys. B 596 (2001) 33-65, Nucl.Phys.B 605 (2001) 647-647 (erratum)

- Double Distribution representation

  Mueller, Robaschik, Geyer, Dittes, Horejsi, Fortsch. Phys. 42 (1994) 101-141

Dyson-Schwinger Equation approach: Zhang et al, Phys. Lett. B 815 (2021) 136158. José Manuel Morgado Chávez, et al, Phys. Rev. Lett. 128 (2022) 20, 202501. Raya et al, Chin. Phys. C 46 (2022) 1, 013105. Xu et al, Chin. Phys. Lett. 40 (2023) 4, 041201. Xu et al, arXiv: 2311.14832. Xing, Ding, Raya, Chang, arXiv: 2301.02958.

Summary and Outlook

Summary

- Form factor: the closest thing we have to a snapshot, the size, shape and makeup of pion
  Electromagnetic form factor, Two-photon transition form factor, Gravitational form factor
- 1D picture of how quarks move within pion
  Parton distribution amplitude, Parton distribution function (PDF) - future experiments (JLab 22 GeV, COMPASS++/AMBER, EIC, EicC) will provide higher precision measurements
- A multidimensional view of pion structure
  Transverse momentum dependent distribution function (TMD), Generalized parton distribution (GPD)

Outlook

- Transverse momentum dependent distribution function (TMD):
  3D images of hadron, Wilson line is essential to any nonzero result for T-odd TMDs.
- Fragmentation function:
  dynamical confinement, critical to extracting TMD from data.

Thank you!